The Journal of Infectious Diseases

MAJOR ARTICLE

Hyperendemicity of Rift Valley Fever in Southwestern Uganda Associated With the Rapidly Evolving Lineage C Viruses

Barnabas Bakamutumaho,[1] John Juma,[2] Erin Clancey,[3,4] Luke Nyakarahuka,[1,5] Silvia Situma,[3,4,6] Raymond Odinoh,[3,4,6] Jeanette Dawa,[3,4,6] Carolyne Nasimiyu,[3,4,6] Evan A. Eskew,[7] Stephen Balinandi,[1] Sophia Mulei,[1] John Kayiwa,[1] John D. Klena,[8] Trevor R. Shoemaker,[8] Shannon L. M. Whitmer,[8] Joel M. Montgomery,[8] John Schieffelin,[9] Julius Lutwama,[1] Allan Muruta,[10] Henry Kyobe Bosa,[10] Scott L. Nuismer,[7] Samuel O. Oyola,[2] Robert F. Breiman,[5,11] and M. Kariuki Njenga[3,4,6]

[1]Uganda Virus Research Institute, Entebbe, Uganda; [2]Genomics Program, International Livestock Research Institute, Nairobi, Kenya; [3]Center for Research in Emerging Infectious Diseases-East and Central Africa, Nairobi, Kenya; [4]Paul G. Allen School of Global Health, Washington State University, Pullman, Washington, USA; [5]Rollins School of Public Health, Emory University, Atlanta, Georgia, USA; [6]Washington State University Global Health-Kenya, Nairobi, Kenya; [7]Department of Biological Sciences, University of Idaho, Moscow, Idaho, USA; [8]Virus Special Pathogens Branch, US Centers for Disease Control and Prevention, Atlanta, Georgia, USA; [9]School of Medicine, Tulane University, New Orleans, Louisiana, USA; [10]Communicable Diseases Department, Uganda Ministry of Health, Kampala, Uganda; and [11]Infectious Diseases and Oncology Research Institute, University of the Witwatersrand, Johannesburg, South Africa

Background. Recent Rift Valley fever (RVF) epidemiology in the eastern Africa region is characterized by widening geographic range and increasing frequency of small disease clusters. Here we conducted studies in the southwestern (SW) Uganda region that has since 2016 reported increasing RVF activities.

Methods. A 22-month long hospital-based study in 3 districts of SW Uganda targeting patients with acute febrile illness or unexplained bleeding was followed by a cross-sectional population-based human-animal survey. We then estimated RVF virus (RVFV) force of infection and yearly cases using age-structured seroprevalence data and conducted genomic phylodynamic modelling of RVFV isolates.

Results. Overall RVF prevalence was 10.5% (205/1968) among febrile or hemorrhagic cases, including 5% (100/1968) with acute (PCR or IgM positive) infection, averaging 5 cases per month. Community-based seroprevalence of 11.8% (88/743) among humans and 14.6% (347/2383) in livestock was observed. Expected yearly human RVF cases were 314–2111 per 1369 km^2 in SW Uganda, up to 3-fold higher than the 0–711 yearly cases in comparable regions of Kenya and Tanzania. Viral genomic studies identified RVFV lineage C, subclade C.2.2 as the circulating strain in SW Uganda since 2019. Lineage C strain has undergone recent rapid evolution and clonal expansion resulting in 4 subclades, C.1.1, C.1.2, C.2.1, and C.2.2, that are adept at establishing endemicity in new territories.

Conclusions. We demonstrate an atypical RVF hyperendemic region in SW Uganda characterized by sustained human clinical RVF cases, unusually high population prevalence, and high number of expected yearly human cases, associated in part with emergence of new RVFV sublineages.

Keywords. Rift Valley fever; interepidemic period; sustained clinical cases; force of infection; lineage C virus.

Rift Valley fever virus (RVFV) was first detected in Kenya in 1931, and subsequently across most countries in Africa over the next 70 years, resulting in severe human and livestock epidemics and serological evidence of endemicity in more than 30 countries [1–3]. In 2000, a severe RVF epidemic occurred in Saudi Arabia and Yemen in the Middle East, associated with livestock trade from the horn of Africa [4]. Once introduced to a country, this mosquito-borne virus becomes endemic in geographic areas supportive of virus maintenance; areas characterized by certain soil types, low elevation, and low annual rainfall [5, 6]. In endemic countries, periodic epidemics, precipitated by heavy rainfall and flooding, are followed by long (4 to > 10 years) interepidemic periods (IEPs) with minimal disease activity [7, 8].

Studies in East Africa have highlighted 2 mechanisms associated with RVFV maintenance and disease burden during IEPs [9–12]. Apart from transovarial virus maintenance and transmission in mosquito eggs, RVFV is also maintained by continuous low-level circulation among wildlife, livestock, humans, and mosquitoes [10]. It is likely that dominance of this cryptic

Received 25 January 2025; editorial decision 31 July 2025; accepted 02 August 2025; published online 6 August 2025

Presented in part: 4th Centre for Research in Emerging Infectious Diseases Annual Conference, 2024, North Carolina, Research Triangle Institute, 10-14 June 2024.

Correspondence: M. Kariuki Njenga, PhD, Paul Allen School for Global Health, Washington State University, 101 Allen Center, Pullman, WA 99164 (Makriuki.njenga@wsu.edu).

The Journal of Infectious Diseases® 2026;233:e77–88

© The Author(s) 2025. Published by Oxford University Press on behalf of Infectious Diseases Society of America.

This is an Open Access article distributed under the terms of the Creative Commons Attribution-NonCommercial-NoDerivs licence (https://creativecommons.org/licenses/by-nc-nd/4.0/), which permits non-commercial reproduction and distribution of the work, in any medium, provided the original work is not altered or transformed in any way, and that the work is properly cited. For commercial re-use, please contact reprints@oup.com for reprints and translation rights for reprints. All other permissions can be obtained through our RightsLink service via the Permissions link on the article page on our site—for further information please contact journals.permissions@oup.com.

https://doi.org/10.1093/infdis/jiaf417

Downloaded from https://academic.oup.com/jid/article/233/1/e77/8222754 by guest on 20 January 2026

cycling is responsible for the changing epidemiology of RVF disease, which is characterized by a growing number of small RVF disease clusters (< 5 human, < 20 livestock cases) that occur across broader agroecological zones [13]. Unlike major regional epidemics, which are often associated with El Niño Southern Oscillation-related extreme weather conditions, the small disease clusters during the IEP ebb and flow in response to routine seasonal variation [11–14].

Within eastern Africa, Kenya and Tanzania documented RVF endemicity decades ago and have been subjected to multicountry epidemics that also involved Somalia and Sudan, most recently in 1997–1998 and 2006–2007 [6, 15]. However, Uganda was not affected by these epidemics, reporting no human RVF cases even with the global and regional public health agencies enhanced surveillance during these epidemics [16]. The situation in Uganda changed in 2016 following confirmation of 2 RVF cases in the southwestern Kabale district [12]. Subsequent investigations detected anti-RVFV immunoglobulin G (IgG) antibodies in 13% of humans and livestock, and infectious virus in mosquitoes collected from the district [12]. Between 2016 and 2023, Uganda reported > 40 small human RVF clusters primarily in the southwestern and central districts [11, 13, 17, 18].

Here, we investigated the epidemiology of RVF in southwestern (SW) Uganda by conducting both a longitudinal hospital-based human study targeting patients with acute febrile illness (AFI) or unexplained bleeding, and a cross-sectional population-based human-animal survey.

METHODS

Study Area and Design

Two studies were conducted in the SW Uganda districts of Isingiro, Kabale, and Rubanda: a hospital-based human prospective study targeting patients ≥ 10 years old with AFI and/or unexplained bleeding, and a cross-sectional community-based human-animal study. The 22-month (September 2021 to July 2023) study enrolled AFI patients at Kabale Regional Referral Hospital in Kabale District, Hamurwa Health Centre in Rubanda District, and Rwekubo Health Centre in Isingiro District. Patients were enrolled if they exhibited undifferentiated fever (> 37.5°C) or a history of fever within the last 4 weeks and a negative malaria test. Additional criteria included unexplained bleeding or severe illness persisting for > 7 days despite treatment. To check coinfection, 20% of the malaria-positive participants were also enrolled. Our target sample size was 707 participants per site assuming a human 8% RVFV prevalence, with 80% power, 2% precision, and a 95% confidence level [12].

The cross-sectional survey was conducted in October to November 2023, using a 2-stage randomization approach. First, 10 subcounties were randomly selected across the 3 districts, and the number of households sampled within each subcounty allocated based on population density [19]. Subsequently, households were selected using randomly generated global positioning system coordinates. At the household, 1 individual aged ≥ 1 year was randomly selected, interviewed, and blood sample collected. For a selected child (aged < 10 years), a parent or guardian was interviewed. For households with livestock, a maximum of 4 animals of each species (goats, cattle, and sheep) were randomly sampled. The target sample sizes, calculated using estimated RVF seroprevalence of 13% in humans, 17.7% in cattle, 3.7% in sheep, and 4.5% in goats, and factoring a 10% household nonresponse rate, was 982 humans and 2476 livestock [12].

Data and Sample Collection

After consenting, participants were clinically examined and both clinical, demographic, and risk factor data electronically collected in Research Electronic Data Capture (REDCap) software [20]. Approximately 5 mL of whole blood were collected from each participant. Harvested sera and blood clots were aliquoted and shipped to Uganda Virus Research Institute and stored at −80°C for subsequent serological and molecular testing.

RVFV Nucleic Acid Detection

Viral RNA was detected from serum using a previously published protocol [21]. Briefly, RNA was extracted using the MagMAX magnetic bead system (Life Technologies) and amplification conducted using the following primer and probe set: 5′-TGAAAATTCCTGAGACACATGG-3′ (RVFL-2912fwdGG), 5′-ACTTCCTTGCATCATCTGATG-3′ (RVFL-2981revAC), and FAM-5′-CAATGTAAGGGGCCTGTGTGGACTTGTG-3′-BHQ (RVFL-probe-2950), on an ABI Quant Studio 5 real-time polymerase chain reaction (PCR) platform (Thermofisher Scientific).

Anti-RVFV Antibody Detection

Sera were screened for total anti-RVFV antibodies (IgM and IgG) using a previously described protocol [12]. Briefly, heat- and detergent-inactivated sera were screened for RVFV total antibodies using a competition multispecies test designed to detect antibodies directed against the RVFV nucleoprotein in serum and plasma. The titers and the cumulative sum of optical densities for each dilution (SUMOD) minus the background absorbance of uninfected control antigen (adjusted SUMOD) were recorded. Samples were considered positive if the titer was 1:400 or above and the adjusted SUMOD and titer exceeded preestablished conservative cutoff values of ≥ 0.45 for IgM enzyme-linked immunosorbent assay (ELISA) and ≥ 0.95 for IgG ELISA.

Estimating RVFV Force of Infection in SW Uganda

To compare the burden of RVFV infection in SW Uganda with adjacent regions, we compared age-stratified RVF population prevalence from our study (excluding hospital study) with 4

Downloaded from https://academic.oup.com/jid/article/233/1/e77/8222754 by guest on 20 January 2026

similar studies previously conducted in Kenya and Tanzania [13, 22, 23]. Each study collected data on individual age, RVFV serological status, and geographic location. Individuals were assigned to 20 arcminute grid cells (roughly 37 km × 37 km in our study region) that encompassed our study region. Seventy-five grid cells containing serological data from at least 20 individuals were used as cutoff for inclusion. These gridded serosurvey data were used to perform 3 analyses: (1) force of infection (FOI) for each grid cell using the age-structured serosurvey data; (2) fit 2 gamma density functions to the FOI estimates, 1 for grid cells within the study area; and (3) used FOI estimates to calculate expected number of yearly RVF cases in each grid cell.

Estimating FOI

We estimated FOI for each grid cell using maximum likelihood, assuming (1) the FOI was constant over time and across age classes; (2) disease-specific mortality was negligible; and (3) that seroreversion was negligible [22, 24]. The proportion of the population in each age class, a, that was seropositive, was described by the following function:

$$P(a) = 1 - exp\{-\lambda a\}, \quad (1)$$

where a was measured in years and λ is the FOI. The likelihood of observing x_i seroprositive individuals with corresponding age class i and $1 - x_i$ seronegative individuals in age class i across age classes was:

$$\mathcal{L}(\lambda) = \prod_{i=1}^{n} P(a_i)^{x_i}(1 - P(a_i))^{|x_i - 1|} \quad (2)$$

where x_i is the serostatus $\{0, 1\}$ of individual i and a_i is the age class, in years, of the ith individual. We maximized the negative logarithm of Equation (2) with respect to λ in R using a variant of simulated annealing within the built-in function "optim" [25, 26].

Quantifying Distribution of FOI

To more rigorously compare the distribution of FOI experienced by humans within SW Uganda to that experienced elsewhere in Tanzania and Kenya, we fit gamma density functions to the FOI data for each study region. Specifically, we used maximum likelihood to estimate the shape (α) and rate (β) parameters for gamma distributions fit to: (1) the FOI estimated for grid cells in Uganda, and (2) the FOI estimated for grid cells in Kenya and Tanzania. Using the simulated annealing in "optim" and estimated shape and rate parameters, we calculated the mode of the gamma distribution in each case as

$$Mode(\lambda) = \begin{cases} 0, & |\alpha < 1 \\ \dfrac{\alpha - 1}{\beta}, & |\alpha \geq 1 \end{cases}.$$

Estimating Expected Yearly RVF Case Counts

Expected RVF case counts were calculated by multiplying the FOI for each grid cell with the estimated population of seronegative humans in that cell. Human population estimates were downloaded from the WorldPop dataset (https://hub.worldpop.org/) of 2020 (most recent) [27], converting density data to human population counts, and then aggregating the count data to the 20 arcminute grid cell size. All manipulation of raster data used functions from the *terra* R package [28].

Whole-Genome Sequencing and Phylogenetic Analysis of RVFV Isolates

High throughput next-generation sequencing was performed on 4 of the 10 RVF PCR-positive samples with cycle threshold (Ct) ≤ 25 (samples CD300/Kabale1-2022, CD301/Rubanda1-2022, CD304/Rubanda2-2023, and CD532/Isingiro1-2023) using a protocol described previously [29–31]. Briefly, RNA was extracted from blood or serum using 5X Magmax 96 Viral Isolation kit and libraries prepared following unbiased shotgun method. Samples were sequenced using RVFV-specific primers designed from Uganda-specific RVFV sequences and the ARTIC protocol [29, 30]. Consensus genome sequences were constructed using the ARTIC bioinformatics protocol using RVFV-specific config files to a RVF reference genome sequence (GenBank accession No. MG972978).

Genomic Data Retrieval, Filtering, and Lineage Assignment

Publicly available RVFV sequence data from the National Center for Biotechnology Information (NCBI) database (search limited to Uganda) were combined with data generated from this study [32]. We successfully retrieved genomic sequence data for the 3 fragments: S (n = 33), M (n = 24), and L (n = 30). For each segment sequence dataset, we determined RVFV lineages using the lineage assignment tool [33].

Phylogenetic Analysis

Multiple sequence alignment of each dataset was performed using MAFFT [34], followed by manual editing using Aliview [35] for correct codon alignment. We inferred the best substitution models using ModelTest-NG [36] and identified HKY + G4, GTR + I, GTR + G4 as optimal for the S, M, and L segments, respectively. We incorporated these evolutionary models in maximum likelihood phylogenetic tree inference using IQ-TREE [35] while estimating branch support values using ultrafast bootstrapping procedure (-bb 1000). To deduce the temporal signal of the sequence data, we regressed the genetic distances and the sampling dates (in years) through a root-to-tip plot (Supplementary Figure 1). We further utilized the sampling dates to compute time-scaled phylogenetic trees using TreeTime [37]. Our root-to-tip reconstructions indicated that the L segment data contained sufficient temporal signal (correlation coefficient = 0.99 and $R^2 = 0.99$) to warrant Bayesian inference. We therefore used the L segment sequence data to perform phylogeographic analysis. To deduce the spatial diffusion of RVFV in Uganda, we utilized continuous phylogeographic reconstruction in BEAST [38], with incorporation of uncorrelated log-normal

Downloaded from https://academic.oup.com/jid/article/233/1/e77/8222754 by guest on 20 January 2026

A

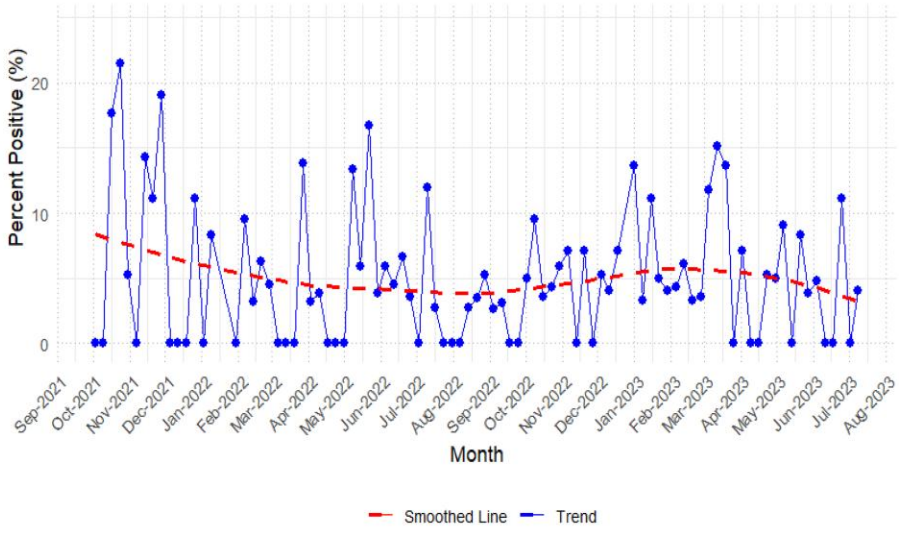

B

Characteristics	Number (total=100)
Fever	92
Headache	84
Joint pains	64
Chills	61
Fatigue/weakness	53
Dizziness	40
Eye pain	19
Drowsiness	17
Bleeding nose/gums	10
Blurry vision	7
Neck stiffness/pain	6
Insomnia	5
Paralysis	4
Jaundice	1

Figure 1. Epicurve (*A*) and clinical characteristics (*B*) of acute Rift Valley fever cases detected at 3 health facilities in southwestern Uganda between September 2021 and July 2023 (n = 100).

tree branching and skyline coalescent demographic models. Using *tidygeocoder* [38], we geocoded the geographical sampling locations into longitude and latitude and used the coordinates as traits in a Cauchy distribution model for continuous phylogeographic inference. BEAST was run with 100 million Markov chain Monte-Carlo steps, sampling every 10 000th step. Effective sample size values (> 200) were assessed using Tracer [39] to ensure proper convergence and mixing of the outputs. We used Tree Annotator [40] to retrieve and annotate the maximum clade credibility tree. We extracted the spatial-temporal information embedded in these phylogeographically reconstructed trees using the *seraphim* package in R [39] to ascertain RVFV transmission in Uganda.

Ethical and Administrative Approvals

Ethical approvals for this study were provided by the Uganda Virus Research Institute Research Ethics Committee (study No. GC/127/849) and the Uganda National Council for Science and Technology (study No. HS1713ES). The study was performed in accordance with the principles of Good Clinical Practice following the Tri-Council guidelines. Written informed consent was obtained from all the study participants.

RESULTS

Sustained Detection of Acute RVF Cases in SW Uganda

Overall, 2711 participants were enrolled in both the hospital-based (n = 1968) and cross-sectional community (n = 743) studies. Between October 2021 and July 2023 (22 months), a total of 1968 febrile patients were enrolled at 3 health facilities located in Isingiro, Kabale, and Rubanda districts, out of which 100 (5.1%) were clinically positive by either viral RNA (n = 6), antiviral IgM antibodies (n = 90), or both (n = 4). Of these 100 clinically positive participants, 90 were managed as outpatients while 10 had severe disease requiring hospitalization. The major clinical manifestations included fever (92%), headache (84%), joint pains (64%), chills (61%), fatigue/weakness (53%), and bleeding (10%) (Figure 1). None of the participants died. Interestingly, there was sustained detection of clinical RVF cases throughout the 22-month period, averaging 5 (range, 1–13) cases per month, but ranging between 0% and 20% of AFI patients weekly as illustrated in Figure 1. No clinically positive RVF cases (viral RNA or IgM positive) were detected in the cross-sectional study (n = 743) conducted across the 3 districts.

Human and Livestock RVF Seroprevalence

Of the 2711 human participants tested for RVFV RNA, IgM, or IgG antibodies, 293 (10.8%) were positive in 1 of these tests, including 205 of 1968 (10.4%) from the prospective hospital-based study and 88 of 743 (11.8%) from the cross-sectional study. We observed clustering of acute cases near the 3 hospitals where surveillance was conducted (Figure 2*A* and 2*B*, red dots), whereas the distribution of IgG-positive participants was more widespread across the 3 districts (Figure 2*B*, green dots). Of 2383 livestock tested from the cross-sectional study, 347 (14.6%) were positive for anti-RVF IgG antibodies, including a significantly higher ($P < .05$) seroprevalence in cattle (33.8%, 230/681) than in goats (6.7%, 78/1170) or sheep (7.3%, 39/532).

Downloaded from https://academic.oup.com/jid/article/233/1/e77/8222754 by guest on 20 January 2026

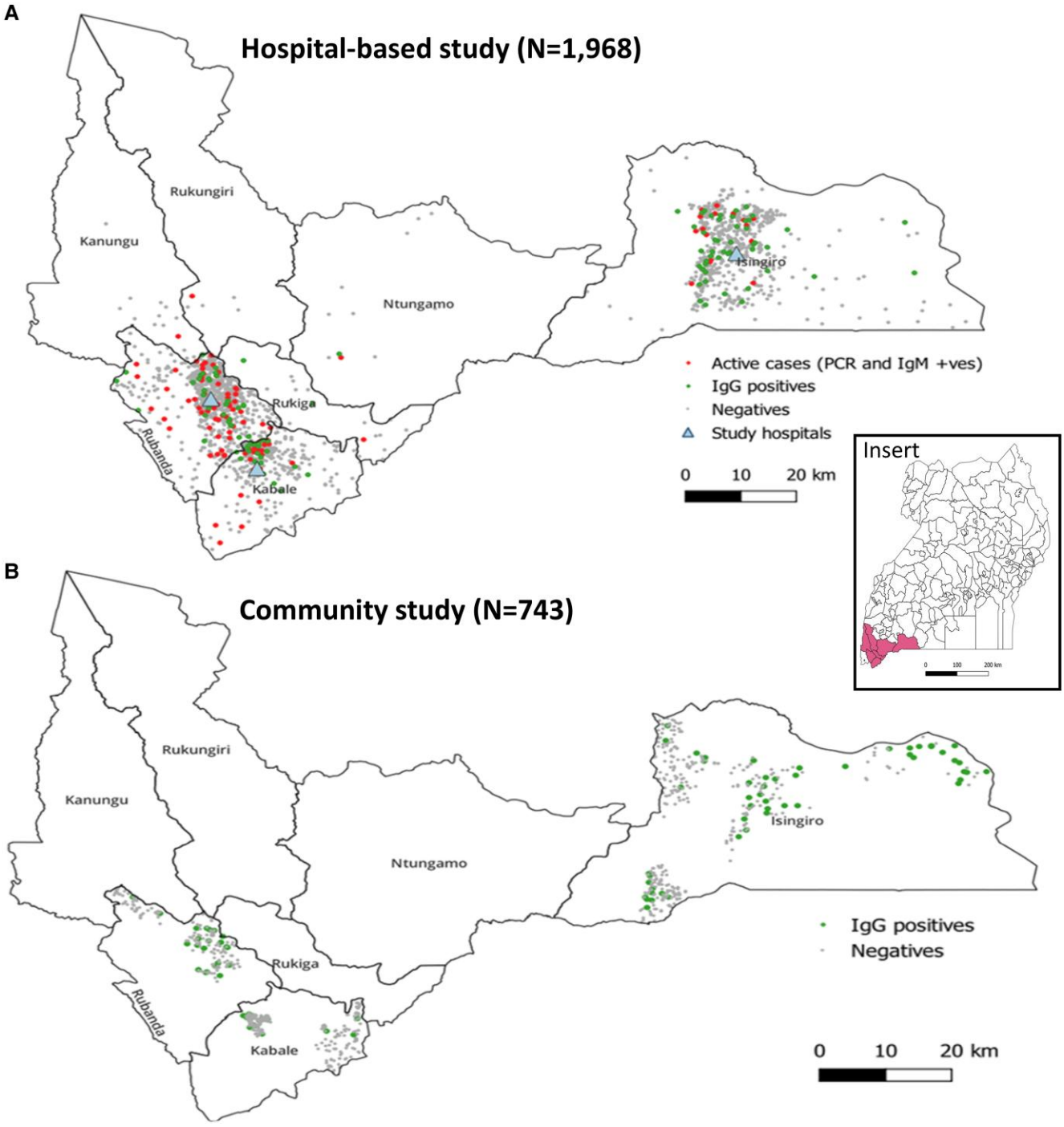

Figure 2. Spatial distribution of human acute and older RVF cases detected in the hospital-based and community studies. RVF acute (PCR or IgM positive) cases (red circles) older (IgG positive) cases (green circles) as detected in the hospital-based (n = 1968) (*A*) and cross-sectional community (n = 743) (*B*) studies in the southwestern Uganda region. The RVF-negative cases are shown as grey circles in both studies. Insert, map of Uganda showing the southwestern Uganda region. Abbreviations: IgM, immunoglobulin M; PCR, polymerase chain reaction; RVF, Rift Valley fever.

RVFV Force of Infection and Expected Yearly RVF Cases

To determine the burden of RVFV infection in the region, we compared the FOI at our study sites to that of adjacent regions in Kenya and Tanzania, using data compiled from previous serosurveys [13, 22, 23]. Although the range of FOI estimates was similar between the 2 regions, the distributions differed (Figure 3*A*), as did the expected yearly RVF cases (Figure 3*B*). Specifically, fitting gamma density functions to the FOI estimates revealed a modal value of 0.00096 infections per year per susceptible individual in SW Uganda but 0 in

Downloaded from https://academic.oup.com/jid/article/233/1/e77/8222754 by guest on 20 January 2026

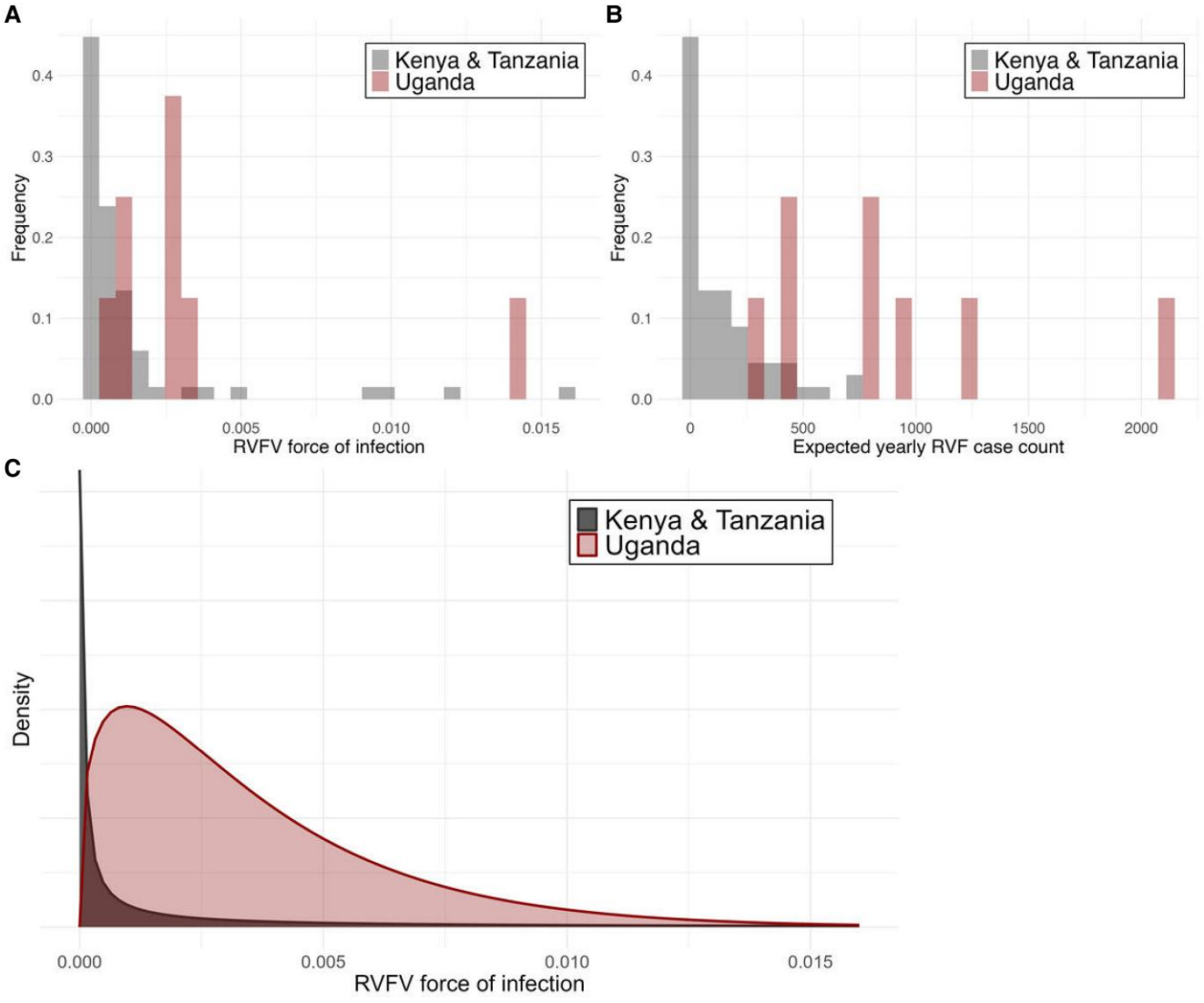

Figure 3. Frequency distribution of Rift Valley fever virus (RVFV) force of infection expressed as infections per year per susceptible individual (*A*), expected yearly RVF cases per grid cell (*B*), and gamma density functions fit to the force of infection estimates (*C*). The gamma density functions fit to force of infection estimates from each region show that the characteristics of the distributions are different, driven by consistent virus circulation during interepidemic periods in southwestern Uganda, and minimal circulation in adjacent regions of Kenya and Tanzania.

Kenya and Tanzania (Figure 3*C*). This difference in the shape of the distributions showed that most human populations in SW Uganda were exposed to RVFV whereas those outside the region were not exposed to RVFV. These results are consistent with widespread, sustained circulation of low-to-medium levels of RVF disease in SW Uganda but isolated and sporadic episodes of intense RVFV infection in Kenya and Tanzania.

After transforming estimated FOI to expected RVF case counts in each grid cell (1369 km^2), we estimated that the SW Uganda region could expect 314–2111 yearly RVF cases per grid cell, whereas the Kenya and Tanzania region could expect 0–711 yearly RVF cases per grid cell (Figure 4).

Circulating RVFV Lineages

From the 10 PCR-positive samples, whole-genome sequencing was successful for 4 samples: 2 from the Rubanda and 1 each from Isingiro districts and Kabale districts (Supplementary Table 1). The samples were collected between 3 October 2022 and 30 January 2023, from male participants, 26–30 years old. The S (nonstructural genes), M, and L segments of the isolates aligned with RVFV lineage C, subclade 2.2 (Figure 5 and Supplementary Tables 2, 3, and 4).

In the RNA-dependent RNA polymerase (RdRp) and glycoprotein genes, we identified 110 and 80 single nucleotide polymorphisms (SNPs), respectively, which were specific to the subclade C.2.2. In addition, 23 defining SNPs in each of

Downloaded from https://academic.oup.com/jid/article/233/1/e77/8222754 by guest on 20 January 2026

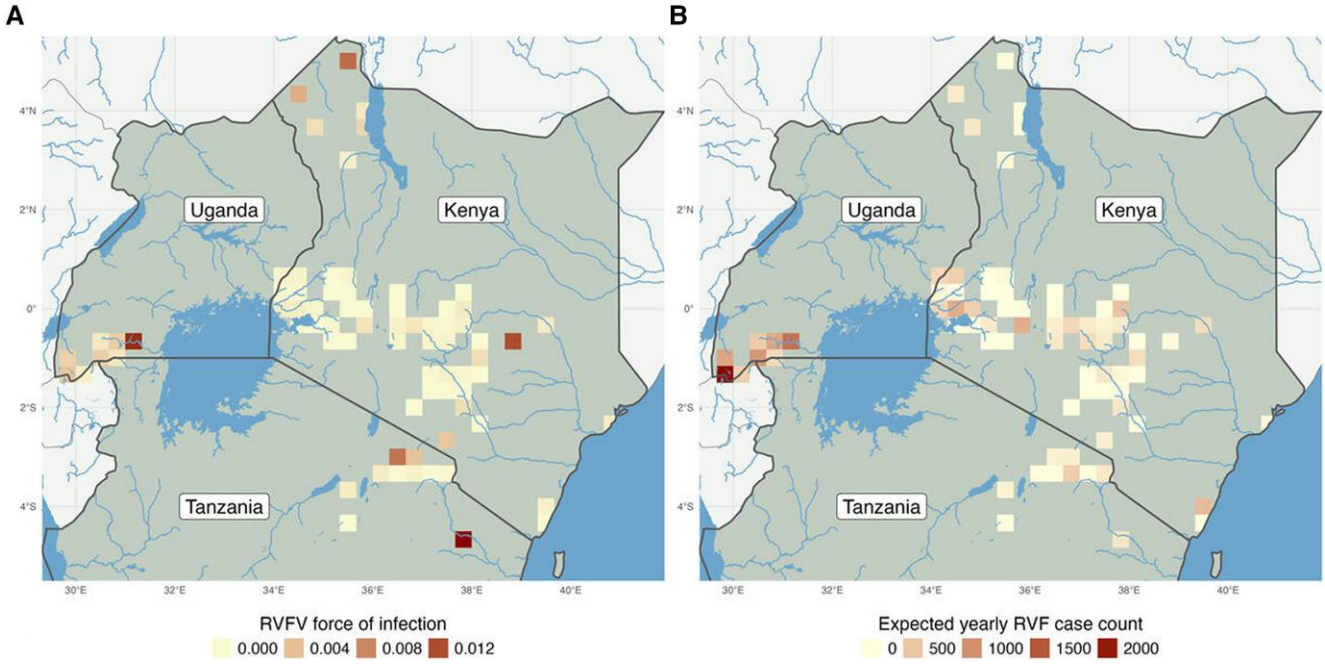

Figure 4. Estimated Rift Valley fever virus (RVFV) force of infection (FOI) for different spatial locations in Kenya, Uganda, and Tanzania (*A*) and translation into expected yearly RVF cases (*B*). The figure illustrates higher RVF circulation the southwest Uganda region, which has a high FOI and large human population, leading to high expected yearly RVF cases.

nonstructural (NSs) and nucleoprotein genes were identified. The key substitutions in the RdRp, nucleoprotein, glycoprotein, and nonstructural genes are shown in Table 1.

Evolution of RVFV Lineages in Uganda

We examined the evolutionary relationships of RVFV lineages circulating in Uganda using genomic sequence data collected between 1944 and 2023. Maximum likelihood phylogenetic trees showed that between the years 1940 and 2000 the circulating strains were lineages C, K, and M (Figure 5). Phylogenetic inference showed clustering of lineages K and M followed by emergence of lineage C in several parts of the country from around 1990. Lineage C, shown to be predominant in Uganda since 2015, has undergone expansion into distinct sublineages C.2.1 and C.2.2 [14]. Notably, sublineage C.2.1 emerged in the country during the first reported human outbreak in 2016 followed by expansion to sublineage C.2.2. Interestingly, we observed long branches in a cluster of 3 sequences isolated in 2018 belonging to lineage K (here reported as K.1.2) sharing ancestry with the livestock vaccine Smithburn isolated in Entebbe in 1944 (Figure 5). Although there is a huge gap in sampling between 1950s and 2000s (a potential bias) the temporal signals as examined by regressing root to tip genetic distances provided sufficient statistical support for the current Bayesian evolutionary analysis (Supplementary Figure 1).

Phylogeographic Dispersal of RVFV Lineages in Uganda

We established sufficient temporal signal in the large segment sequences and applied continuous phylogeographic analysis to understand the dispersal dynamics of RVFV lineages in Uganda. Although our genomic dataset was limited in terms of the number of sequences sampled (n = 30), the phylogeographic analysis shows that RVFV lineages tended to disperse from the SW Uganda region. The dispersal diffusion of RVFV lineages showed several introductions of the virus through the SW Kabale and Isingiro districts and eastern Busia district (Figure 6). We showed that the time of the most recent ancestor (tMRCA) of RVFV lineages in Uganda may have been over 100 years ago in 1921 (95% highest posterior density [HPD], 1899–1940). The evolution rate of the medium segment is 3.57E-4 (95% HPD, 2.62E-4–4.65E-4) substitutions per site per year. Our continuous phylogeographic analysis aligns well with the patterns of livestock movements in the cattle corridor, which stretches from southwestern to northeastern Uganda.

DISCUSSION

To our knowledge, this is the first study describing an RVF hyperendemic region characterized by sustained detection of human clinical RVF cases visiting hospitals, unusually high population prevalence among humans and livestock, and estimated FOI consistent with high expected annual human RVF

Downloaded from https://academic.oup.com/jid/article/233/1/e77/8222754 by guest on 20 January 2026

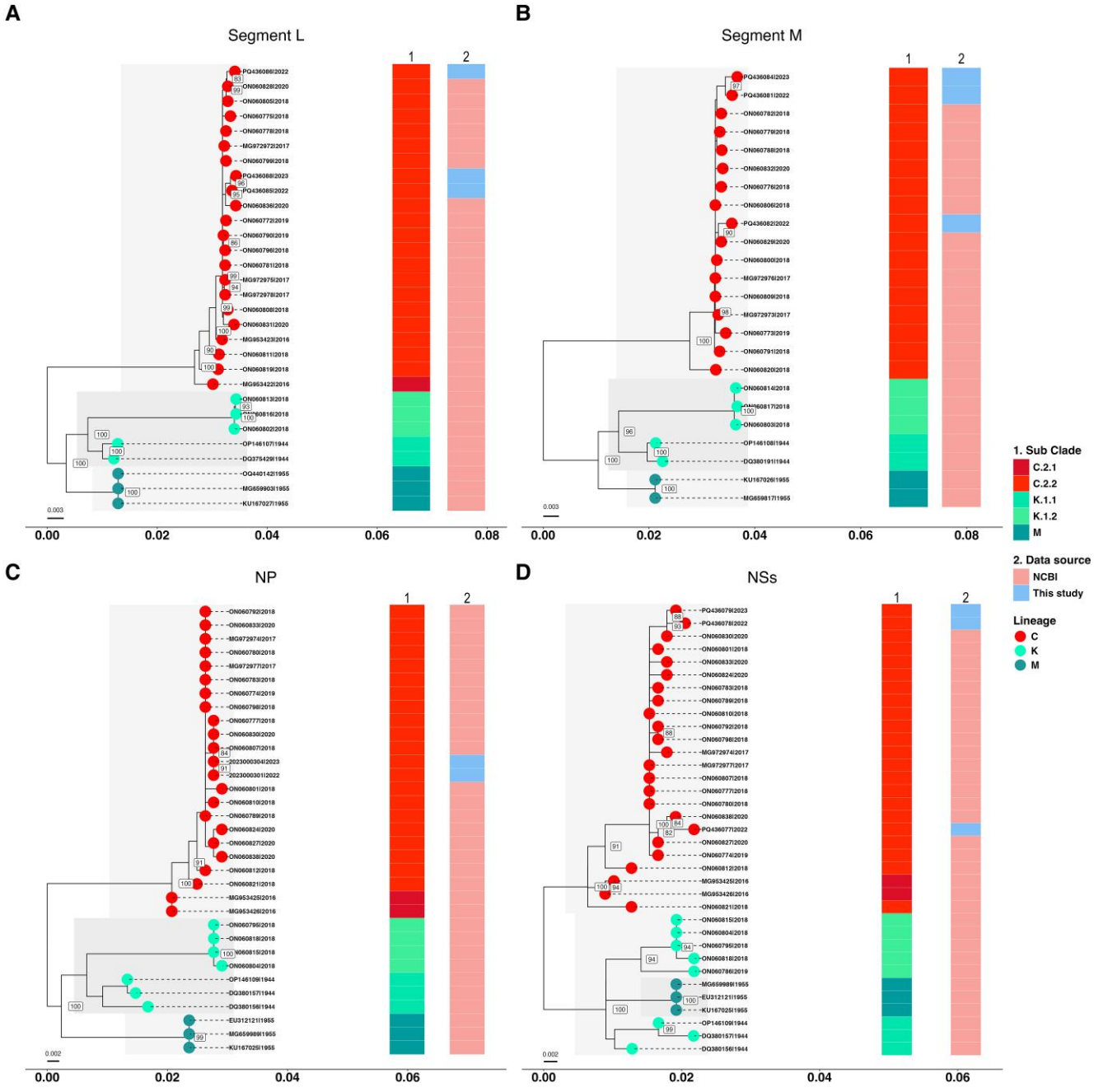

Figure 5. Phylogenetic inference of RVFV lineage evolution in Uganda. Maximum likelihood phylogenetic trees were reconstructed using IQ-TREE: (*A*) L segment (n = 30), (*B*) M segment (n = 24), (*C*) NP (n = 33), and (*D*) NS gene sequences from the S segment. The tips of the trees are colored using the RVFV lineage information from assignment and labelled by accession numbers and sampling dates (year). Statistical support for tree nodes is indicated by bootstrap values. Abbreviations: NCBI, National Center for Biotechnology Information; NP, nucleoprotein; NSs, nonstructural; RVFV, Rift Valley fever virus.

case counts across the region. Over a period of almost 2 years, 5% (100/1968) of patients presenting with AFI or unexplained bleeding at 3 hospitals in SW Uganda were positive for RVF, averaging 4.5 cases per month and up to 20% of febrile cases per week. While none of the patients died, they exhibited classic RVF clinical manifestations, including headache, joint pains, and bleeding syndromes, with 10% requiring hospitalization for intensive clinical care. An additional 5% (105/1968) of the enrolled patients had prior exposure to RVFV, demonstrated by presence of antiviral IgG antibodies, giving an overall RVF disease prevalence of 10.5% (205/1968). As expected, spatial mapping showed clustering of cases around the hospitals, suggesting even more widespread RVFV infection given the challenges associated with seeking health care in rural Africa.

Downloaded from https://academic.oup.com/jid/article/233/1/e77/8222754 by guest on 20 January 2026

Within the community, human and livestock RVFV seroprevalences were 11.8% (88/743) and 14.6% (347/2383), respectively. Our similar studies in the central highlands of Kenya and the eastern Democratic Republic of Congo failed to detect acute RVF cases among AFI patients, while in communities, human and livestock RVFV prevalences were 3–6-fold lower than in SW Uganda [41]. When compared to findings from the randomized population-based seroprevalence studies conducted elsewhere in Africa and the Middle East, the RVFV prevalence in SW Uganda was 2–6-fold higher [22, 41–45]. Comparing the distribution of RVFV FOI estimates between human populations in SW Uganda with adjacent regions in Kenya and Tanzania showed an interior mode of 0.00096 in SW Uganda while it was 0 in other regions, indicating that SW Uganda had persistently nonzero FOI, while most areas in Kenya and Tanzania had zero or near zero FOIs. Overall, these findings confirm the existence of sustained low-to-medium levels of RVF cases in SW Uganda, and likely elsewhere in other countries where the virus is endemic.

Virus genomic evolution and transmission studies showed that the RVFV strains circulating in SW Uganda since 2019, including isolates from the current study, belong to lineage C sublineage C.2.2, which was first detected in Kenya during the 2006–2007 RVF epidemic [33, 46]. Previous studies showed that lineage C is the predominant virus circulating in the eastern Africa region since the 1990s [47]. First detected in Zimbabwe in 1976, lineage C virus was introduced to Kenya, thereafter undergoing clonal expansion during the large

Table 1. Key Substitutions Observed in the RNA-Dependent RNA Polymerase, Glycoprotein, Nucleoprotein, and the Small Nonstructural Gene

Segment	Gene	Substitutions
Large	RNA-dependent RNA polymerase (RdRp)	F23Y, R249K, S278D, S278N, A288V, V302I, V349I, S411N, D446N, S470N, A663T, V1333I, I1773V, K1906R, D1984N
Medium	Glycoprotein	I60V, D95N, L232Q, L368Q, D566G, I631V, S1059T, T1183I
Small	Nonstructural (NSs)	F23I, R24K, Y33F, N133S, T152A, A167V, V217A, I242V, E253G
Small	Nucleoprotein (N gene)	G160E

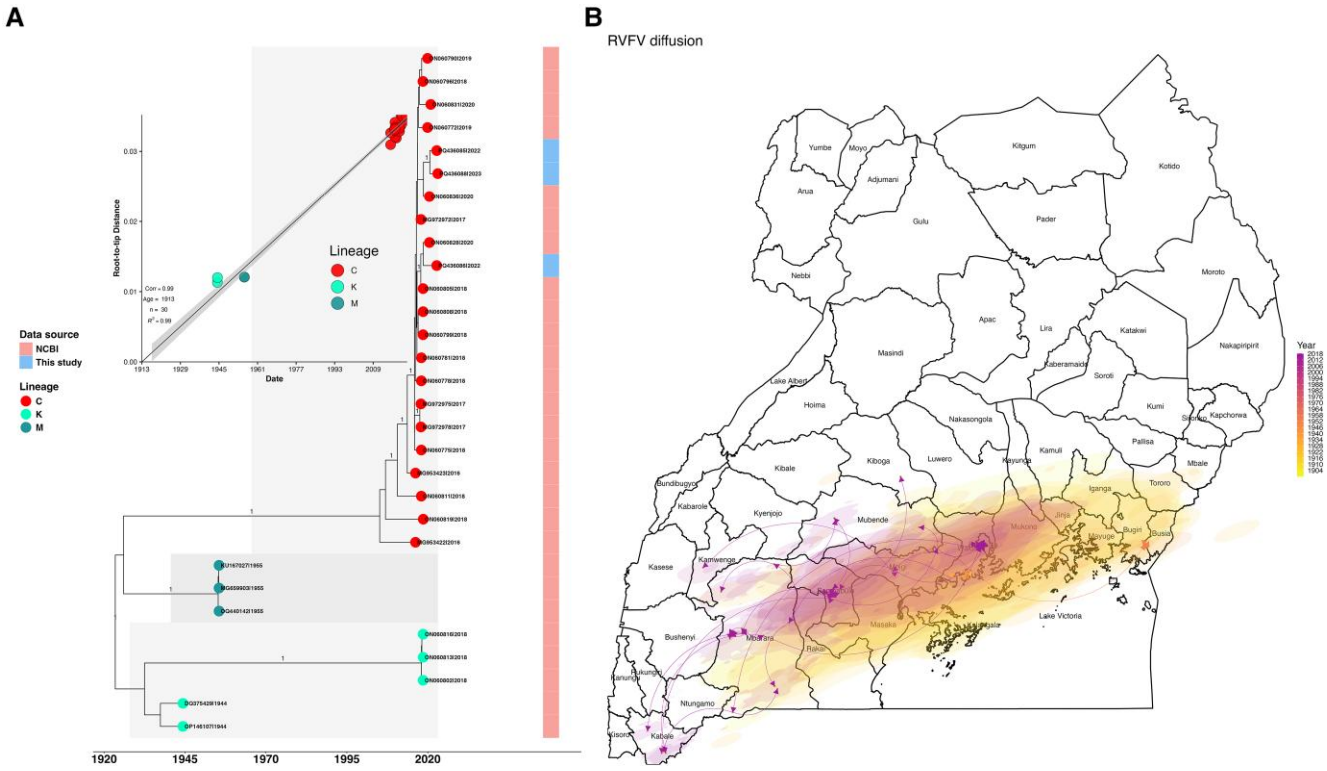

Figure 6. Continuous phylogeographic analysis of RVFV lineages in Uganda using complete L segment sequences (n = 30). Dispersal history of RVFV lineages summarized by an MCC tree retrieved and annotated from 900 posterior trees sampled from the posterior distribution of the continuous phylogeographic analysis. *A*, MCC tree retrieved from the Bayesian phylogenetic inference based on the medium segment genomic sequences and highlighting the clustering of the different lineages of the virus. The tips of the tree are colored according to lineage information and labels show the accession numbers and sampling time in years. *A*, Insert shows root-to-tip plot illustrating regression of the genetic distances and the sampling time (year) of the isolates. *B*, Nodes of the trees are colored according to the time of occurrence, and oldest nodes are plotted on top of youngest ones. The light grey shaded areas in the map depict lakes. Abbreviations: MCC, maximum clade credibility; NCBI, National Center for Biotechnology Information; RVFV, Rift Valley fever virus.

Downloaded from https://academic.oup.com/jid/article/233/1/e77/8222754 by guest on 20 January 2026

2006–2007 epidemic and creating distinct subclusters. Phylogenetic analysis focusing on lineage C indicates a variant undergoing evolution at a relatively increased rate, producing 4 sublineages, C1.1, C1.2, C2.1, and C2.2, attributed to silent circulation during IEPs. Phylogeographic analysis showed the ability of lineage C to establish endemicity in new territories, likely therefore catalyzing the widening geographic range of RVF clusters recently described [13]. Apart from virus strains, other factors that likely contribute to RVF hyperendemicity in SW Uganda include climatic changes and anthropogenic factors such as land use change and environmental degradation [13].

This study had some limitations. In conducting FOI comparisons, we assumed that FOI is constant over time. However, it is highly plausible that FOI can shift over time for a variety of reasons, including changing population immunity. The consequence would be that our FOI estimates was biased (high) because of recent shift in disease dynamic in Uganda. However, the measure allowed us to convert spatially explicit seroprevalence data to a comparable quantitative measure, which is a realistic reflection of the changing disease landscape in Uganda.

Supplementary Data

Supplementary materials are available at *The Journal of Infectious Diseases* online (http://jid.oxfordjournals.org/). Supplementary materials consist of data provided by the author that are published to benefit the reader. The posted materials are not copyedited. The contents of all supplementary data are the sole responsibility of the authors. Questions or messages regarding errors should be addressed to the author.

Notes

Author contributions. B. B., L. N., J. D., R. F. B., and M. K. N. conceived and designed the study. All authors drafted and revised the manuscript, and reviewed and approved the final version. All authors accept responsibility to submit for publication.

Acknowledgments. We thank the Uganda Ministry of Health for administrative approval and the Uganda Virus Research Institute (UVRI) for laboratory support and ethical oversight. We thank Alex Tumusiime, Jackson Kyondo, and Justine Okello for field and diagnostic support, and Angela Ndiu and Stella Nabatanzi for administrative support.

Data availability. All decoded data generated or analyzed in this study will be available upon reasonable request from the corresponding author or first author. GenBank accession numbers for sequences derived in this study are PQ436077 through PQ436088.

Disclaimer. The findings and conclusions in this report are those of the authors and do not necessarily represent the official position of the US Centers for Disease Control and Prevention/Agency for Toxic Substances and Disease Registry or the Uganda Ministry of Health.

Financial support. This work was supported by the US National Institute of Allergy and Infectious Disease/National Institutes of Health (NIAID/NIH) through the Centre for Research in Emerging Infectious Diseases-East and Central Africa (grant number U01AI151799). Genomic work in the laboratory of S. O. O. was supported by the Global Health European Development Countries Clinical Trials Partnership-3 joint undertaking and its members (grant number 101103171); the Bill and Melinda Gates Foundation; and the Rockefeller Foundation. Laboratory testing at UVRI was supported by the US Centers for Disease Control and Prevention (grant to the institute). S. S. received training support from the NIH, Fogarty International Center (grant number D43TW011519 D43 training to Washington State University and University of Nairobi). J. S. was supported by the NIAID, NIH through the West Africa Research Network in Infectious Diseases (grant number 5U01AI151812).

Potential conflicts of interest. All authors: No reported conflicts of interest.

All authors have submitted the ICMJE Form for Disclosure of Potential Conflicts of Interest. Conflicts that the editors consider relevant to the content of the manuscript have been disclosed.

References

1. Daubney R, Hudson J. Enzootic hepatitis or Rift Valley fever. An undescribed virus disease of sheep, cattle and man from East Africa. J Pathol Bacteriol **1931**; 34:545–79.
2. El-Akkad A. Rift Valley fever outbreak in Egypt. October–December 1977. J Egypt Public Health Assoc **1978**; 53: 123–8.
3. Zeller HG, Fontenille D, Traore-Lamizana M, Thiongane Y, Digoutte J-P. Enzootic activity of Rift Valley fever virus in Senegal. Am J Trop Med Hyg **1997**; 56:265–72.
4. Al-Hazmi M, Ayoola EA, Abdurahman M, et al. Epidemic Rift Valley fever in Saudi Arabia: a clinical study of severe illness in humans. Clin Infect Dis **2003**; 36:245–52.
5. Memish ZA, Masri MA, Anderson BD, et al. Elevated antibodies against Rift Valley fever virus among humans with exposure to ruminants in Saudi Arabia. Am J Trop Med Hyg **2015**; 92:739–43.
6. Hightower A, Kinkade C, Nguku PM, et al. Relationship of climate, geography, and geology to the incidence of Rift Valley fever in Kenya during the 2006–2007 outbreak. Am Soc Trop Med Hyg **2012**; 86:373–80.
7. Anyamba A, Chretien J-P, Small J, et al. Prediction of a Rift Valley fever outbreak. Proc Natl Acad Sci **2009**; 106: 955–9.

Downloaded from https://academic.oup.com/jid/article/233/1/e77/8222754 by guest on 20 January 2026

8. Murithi RM, Munyua P, Ithondeka PM, et al. Rift Valley fever in Kenya: history of epizootics and identification of vulnerable districts. Epidemiol Infect **2011**; 139: 372–80.
9. Sindato C, Pfeiffer DU, Karimuribo ED, Mboera LEG, Rweyemamu MM, Paweska JT. A spatial analysis of Rift Valley fever virus seropositivity in domestic ruminants in Tanzania. PLoS One **2015**; 10:e0131873.
10. Kariuki Njenga M, Bett B. Rift Valley fever virus—how and where virus is maintained during inter-epidemic periods. Curr Clin Microbiol Rep **2019**; 6:18–24.
11. Madani TA, Al-Mazrou YY, Al-Jeffri MH, et al. Rift Valley fever epidemic in Saudi Arabia: epidemiological, clinical, and laboratory characteristics. Clin Infect Dis **2003**; 37: 1084–92.
12. Nyakarahuka L, De St. Maurice A, Purpura L, et al. Prevalence and risk factors of Rift Valley fever in humans and animals from Kabale district in southwestern Uganda, 2016. PLoS Negl Trop Dis **2018**; 12:e0006412.
13. Situma S, Nyakarahuka L, Omondi E, et al. Widening geographic range of Rift Valley fever disease clusters associated with climate change in East Africa. BMJ Glob Health **2024**; 9:e014737.
14. Nsengimana I, Juma J, Roesel K, et al. Genomic epidemiology of Rift Valley fever virus involved in the 2018 and 2022 outbreaks in livestock in Rwanda. Viruses **2024**; 16:1148.
15. Nguku PM, Sharif S, Mutonga D, et al. An investigation of a major outbreak of Rift Valley fever in Kenya: 2006–2007. Am J Trop Med Hyg **2010**; 83:05–13.
16. World Health Organization. Outbreaks of Rift Valley fever in Kenya, Somalia and United Republic of Tanzania, December 2006–April 2007. Wkly Epidemiol Rec **2007**; 82:389–400.
17. Kabami Z. Notes from the field: Rift Valley fever outbreak—Mbarara District, western Uganda, January–March 2023. MMWR Morb Mortal Wkly Rep **2023**; 72: 639–40.
18. Aceng FL, Kayiwa J, Elyanu P, et al. Rift valley fever outbreak in Sembabule District, Uganda, December 2020. One Health Outlook **2023**; 5:16.
19. Uganda Bureau of Statistics. National population and household census (NPHC), 2024. https://www.ubos.org/datasets/. Accessed 2 May 2025.
20. REDCap. Software. https://projectredcap.org/software/. Accessed 27 May 2023.
21. Bird BH, Khristova ML, Rollin PE, Ksiazek TG, Nichol ST. Complete genome analysis of 33 ecologically and biologically diverse Rift Valley fever virus strains reveals widespread virus movement and low genetic diversity due to recent common ancestry. J Virol **2007**; 81:2805–16.
22. De Glanville WA, Nyarobi JM, Kibona T, et al. Inter-epidemic Rift Valley fever virus infection incidence and risks for zoonotic spillover in northern Tanzania. PLoS Negl Trop Dis **2022**; 16:e0010871.
23. Cook EAJ, Grossi-Soyster EN, De Glanville WA, et al. The sero-epidemiology of Rift Valley fever in people in the Lake Victoria basin of Western Kenya. PLoS Negl Trop Dis **2017**; 11:e0005731.
24. Heisey DM, Joly DO, Messier F. The fitting of general force-of-infection models to wildlife disease prevalence data. Ecology **2006**; 87:2356–65.
25. Bélisle CJP. Convergence theorems for a class of simulated annealing algorithms on R^d. J Appl Probab **1992**; 29: 885–95.
26. R Core Team. A language and environment for statistical computing. Vienna, Austria: R Foundation for Statistical Computing, **2021**.
27. Tatem AJ. WorldPop, open data for spatial demography. Sci Data **2017**; 4:170004.
28. Hijmans RJ. Terra. Spatial data analysis, CRAN: contributed packages. R Foundation, **2020**. doi: 10.32614/cran.package.terra.
29. Quick J, Grubaugh ND, Pullan ST, et al. Multiplex PCR method for MinION and Illumina sequencing of Zika and other virus genomes directly from clinical samples. Nat Protoc **2017**; 12:1261–76.
30. Kinganda-Lusamaki E, Black A, Mukadi DB, et al. Integration of genomic sequencing into the response to the Ebola virus outbreak in Nord Kivu, Democratic Republic of the Congo. Nat Med **2021**; 27:710–6.
31. Li H. Aligning sequence reads, clone sequences and assembly contigs with BWA-MEM. **2013**. https://doi.org/10.48550/arXiv.1303.3997.
32. O'Leary NA, Wright MW, Brister JR, et al. Reference sequence (RefSeq) database at NCBI: current status, taxonomic expansion, and functional annotation. Nucleic Acids Res **2016**; 44:D733–45.
33. Juma J, Fonseca V, Konongoi SL, et al. Genomic surveillance of Rift Valley fever virus: from sequencing to lineage assignment. BMC Genomics **2022**; 23:520.
34. Katoh K, Standley DM. MAFFT multiple sequence alignment software version 7: improvements in performance and usability. Mol Biol Evol **2013**; 30:772–80.
35. Larsson A. AliView: a fast and lightweight alignment viewer and editor for large datasets. Bioinformatics **2014**; 30: 3276–8.
36. Darriba D, Taboada GL, Doallo R, Posada D. jModelTest 2: more models, new heuristics and parallel computing. Nat Methods **2012**; 9:772.
37. Nguyen L-T, Schmidt HA, Von Haeseler A, Minh BQ. IQ-TREE: a fast and effective stochastic algorithm for

Downloaded from https://academic.oup.com/jid/article/233/1/e77/8222754 by guest on 20 January 2026

estimating maximum-likelihood phylogenies. Mol Biol Evol **2015**; 32:268–74.
38. Suchard MA, Lemey P, Baele G, Ayres DL, Drummond AJ, Rambaut A. Bayesian phylogenetic and phylodynamic data integration using BEAST 1.10. Virus Evol **2018**; 4:vey016.
39. Rambaut A, Drummond AJ, Xie D, Baele G, Suchard MA. Posterior summarization in Bayesian phylogenetics using tracer 1.7. Syst Biol **2018**; 67:901–4.
40. Sagulenko P, Puller V, Neher RA. TreeTime: maximum-likelihood phylodynamic analysis. Virus Evol **2018**; 4: vex042.
41. Situma S, Omondi E, Nyakarahuka L, et al. Serological evidence of cryptic Rift Valley fever virus transmission among humans and livestock in central highlands of Kenya. Viruses **2024**; 16:1927.
42. Al-Azraqi TA, El Mekki AA, Mahfouz AA. Rift valley fever in Southwestern Saudi Arabia: a sero-epidemiological study seven years after the outbreak of 2000–2001. Acta Trop **2012**; 123:111–6.
43. Gudo ES, Pinto G, Weyer J, et al. Serological evidence of rift valley fever virus among acute febrile patients in Southern Mozambique during and after the 2013 heavy rainfall and flooding: implication for the management of febrile illness. Virol J **2016**; 13:96.
44. Johnson SAM, Asmah R, Awuni JA, et al. Evidence of Rift Valley fever virus circulation in livestock and herders in Southern Ghana. Viruses **2023**; 15:1346.
45. Pourrut X, Nkoghé D, Souris M, et al. Rift valley fever virus seroprevalence in human rural populations of Gabon. PLoS Negl Trop Dis **2010**; 4:e763.
46. Grobbelaar AA, Weyer J, Leman PA, Kemp A, Paweska JT, Swanepoel R. Molecular epidemiology of rift valley fever virus. Emerg Infect Dis **2011**; 17:2270–6.
47. Juma J, Tegally H, Konongoi S, et al. Leveraging pathogen genomics and phylodynamic modelling to unravel the evolution and transmission dynamics of Rift Valley fever virus in Africa. SSRN, doi: 10.2139/ssrn.4965921, 25 September 2024, preprint: not peer reviewed.

Downloaded from https://academic.oup.com/jid/article/233/1/e77/8222754 by guest on 20 January 2026